ELLIPTICAL SRF CAVITY DESIGN FOR PEFP EXTENSION*

H. S. Kim#, H. Y. Kwon, J. H. Jang, Y. S. Cho, PEFP, KAERI, Korea

Abstract

To increase the beam energy up to 1 GeV by extending a PEFP 100-MeV proton linac, a study on the superconducting RF linac is underway. SRF technology is chosen due to its operational flexibility and lower beam loss, as well as its high accelerating performance and low operating cost. Preliminary study on the beam dynamics shows that two types of cavity with geometrical beta of 0.50 and 0.74 can cover the entire energy range from 100 MeV to 1 GeV. Assuming the achievable peak surface electric field to be 30 MV/m and 35 MV/m for medium and high beta cavity, respectively, we designed the six-cell elliptical cavities by optimizing the cavity parameters such as peak field ratio, inter-cell coupling and r/Q through the geometrical parameter sweep. The details of the SRF cavity design for PEFP extension will be presented.

SCL FOR PEFP LINAC EXTENSION

The proton linac for PEFP is a 100-MeV machine based on normal conducting technology, which consists of a proton injector, a 3-MeV RFQ and a 100-MeV DTL. To extend the output beam energy to 1 GeV, SRF linac is under consideration [1]. The baseline parameters for PEFP SRF linac for 1-GeV extension are like followings.

- Input proton energy: 100 MeV
- Output proton energy: 1000 MeV
- Peak beam current: 20 mA
- Beam duty factor: 5 %
- Operating frequency: 700 MHz
- RF power source: Inductive output tube (IOT)
- Cavity type: multicell elliptical shape
- Number of cavity group: 2
- Beam focusing: SC solenoid

Beam dynamics study based on the baseline parameters shows that two cavity groups (β_g = 0.50 and β_g = 0.74) can provide the required beam energy of 1 GeV. The cavity geometrical beta can be defined by the cell length of $\beta_g\lambda/2$, where λ is the RF free space wavelength. The operating frequency is determined to be 700 MHz because the operating frequency of the RFQ and DTL is 350 MHz. Beam focusing will be provided by SC solenoid magnets installed between every two cavities to avoid too short cryomodule and to make a round beam shape. An inductive output tube (IOT) is chosen for the RF source due to its low operating voltage and economic reasons. The output RF power of commercially available single IOT is limited to about 150 kW; therefore, two IOTs per cavity are going to be used if the required RF power per cavity is more than 150 kW. No cavity requires more than 300 kW.

CAVITY SHAPE DESIGN

During the elliptical cavity shape design and optimization, several parameters such as the iris radius, the wall inclination angle, the iris ellipse ratio, the equator ellipse ratio or dome radius and the cell radius should be carefully considered. In addition, the mechanical stability is of concern especially for the low-beta pulsed machine. The cavity design criteria are prepared as shown in Table 1, which is not absolute but serves as guidelines for design purpose.

Table 1: Cavity Design Guidelines

Parameter	Range
Epeak	< 30 MV/m
Bpeak/Epeak	~1.8 mT/(MV/m)
Fabrication aspect	Min. radius > 2*wall thickness
BCP&HPR aspect	Wall angle > 6 deg.
Mechanical resonance	Min. eigenfrequency > 60 Hz
Lorentz force detuning	< 4.0 Hz/(MV/m)^2
Tuning sensitivity	< 20 N/kHz
Vacuum loading	Max. von Mises stress < 30 MPa

To meet the design requirements, several iterations with varying the geometry of the cavity shape were performed. The equator ellipse ratio has negligible effect on the RF properties of the cavity unless it is too large enough to cause problems on mechanical stability. Therefore it is set to be 1 for the medium beta cavity and 1.2 for the high beta cavity to make it easy to tune the end cell. The dependency of the cavity parameters such as peak field ratio, inter-cell coupling and r/Q on the iris radius is shown in Fig. 1. The smaller iris radius preferred as far as the inter-cell coupling is acceptable. Figure 2 shows the peak field ratio variation due to the wall angle change. The large wall angle makes the surface treatment more convenient and the surface electric field lower. However, the peak surface magnetic field increases and inter-cell coupling decreases as the wall angle increases. The wall distance of the cavity wall from the iris plane determines the electric and magnetic peak fields on the cavity wall and the larger wall distance results in lower peak electric field ratio and higher peak magnetic field as shown in Fig. 3. With chosen geometrical parameters through the above considerations, the iris ellipse ratio can be determined to give the lowest surface electric field as shown in Fig. 4. The designed cavity geometry for the medium beta and the high beta cavity is shown in Fig. 5.

*Work supported by MEST of the Korean Government
#kimhs@kaeri.re.kr

ISBN 978-3-95450-115-1

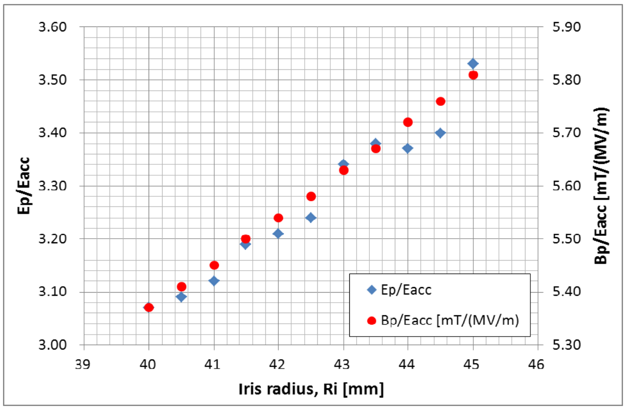

(a) Surface peak field ratio

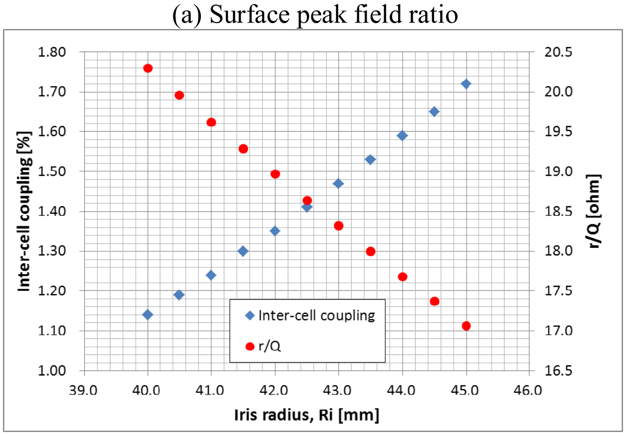

(b) Inter-cell coupling and r/Q

Figure 1: Dependency on the iris radius.

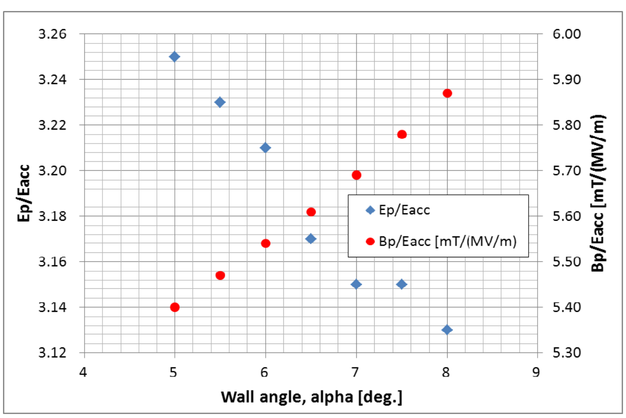

Figure 2: Peak surface field dependence on wall angle.

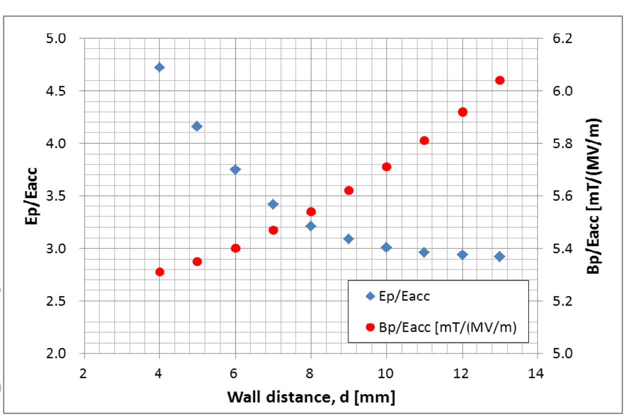

Figure 3: Peak surface field dependence on wall distance.

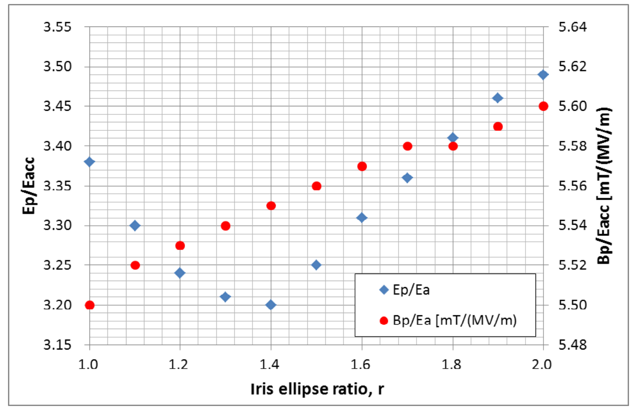

Figure 4: Peak field dependence on the iris ellipse ratio

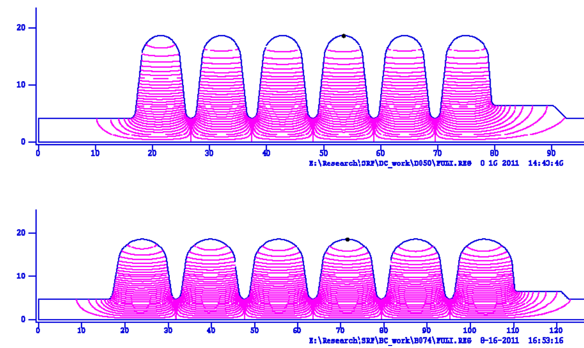

Figure 5: Designed cavity shape. upper: medium beta cavity, lower: high beta cavity.

STATIC LORENTZ DETUNING

We performed the mechanical analysis by using the SuperFish and ANSYS code. Basic procedure of the analysis is given in Reference [2]. ANSYS model was generated based on the SuperFish mesh data. After the ANSYS mechanical analysis with the radiation pressure on each node, which is extracted from the SuperFish output data, the resulting displacement information was transferred to the SuperFish input file. By using this procedure, the original shape and deformed one share the same nodes, which guarantee the accuracy of the frequency shift calculation.

Figure 6 shows the radiation pressure distribution along the cavity. The pressure direction around the equator region, where the magnetic field is dominant is outward and around the iris region, where electric field is dominant is inward. Therefore the radiation pressure tends to decrease the resonant frequency. By using the stiffening ring between the cells as shown in Fig. 7, the deformation and the frequency shift can be reduced.

The analysis results are shown in Fig. 8. With the stiffening ring at 70 mm from beam axis, the Lorentz detuning coefficient is estimated about 6.02 Hz/(MV/m)^2 when the wall thickness is 4.0 mm. If we increase the wall thickness to 4.3 mm, the value is lower to 5.66 Hz/(MV/m)^2. These values are larger than the value of guideline given in Table 1. In the previous study on low beta cavity ($\beta_g = 0.42$), the double stiffening structure was proposed and the Lorentz detuning coefficient can be lower below 1 Hz/(MV/m)^2 [3]. However, if the double stiffening structure is adopted, the cavity is much stiffer and the tuning is difficult during both the field flatness tuning and the normal operation. It is considered to require more study on this aspect.

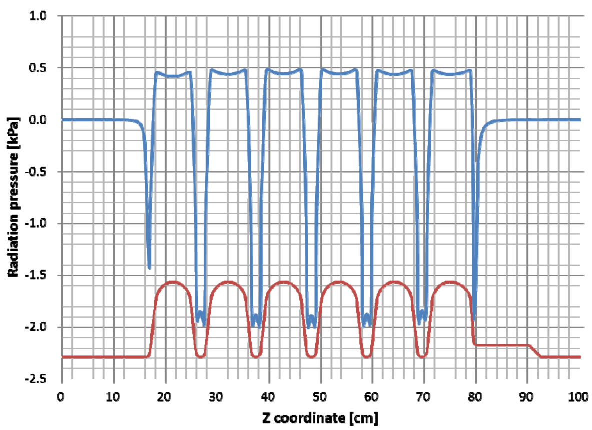

Figure 6: Radiation pressure distribution along the cavity.

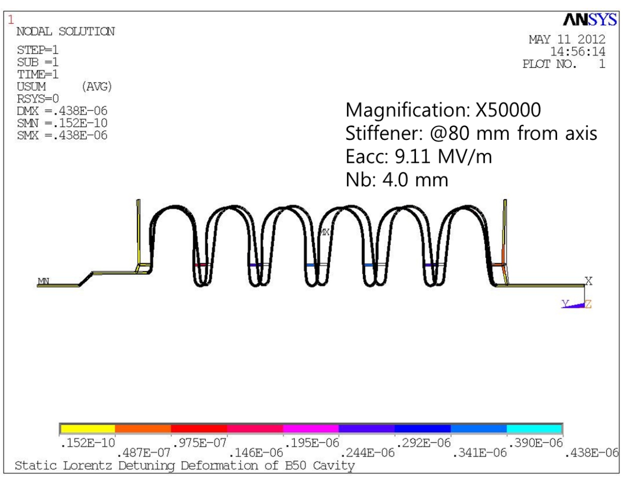

Figure 7: Cavity deformation due to radiation pressure.

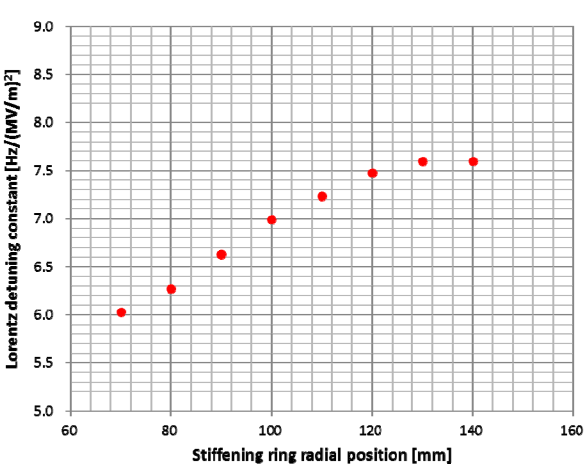

Figure 8: Lorentz force detuning coefficient as a function of stiffening ring radial position.

MULTIPACTING ANALYSIS

For the designed cavity, the multipacting analysis was performed by using the Multipac2.1 code [4]. For multipacting to occur, two conditions must be met; one is the resonant trajectory condition and the other is the impact energy condition. In this analysis, we assumed that the secondary electron yield is larger than one in the impact energy range between 45 eV and 1600 eV and maximum yield is 1.5 around 360 eV. The enhanced counter function which accounts for the electron multiplication is shown in Fig. 9. As shown in Fig. 9 and 10, even though the resonant condition of 1st order two-point trajectory can be met with the peak electric field around 33 MV/m near the equator region, multipacting is not likely to be of concern because the electron impact energy is too low.

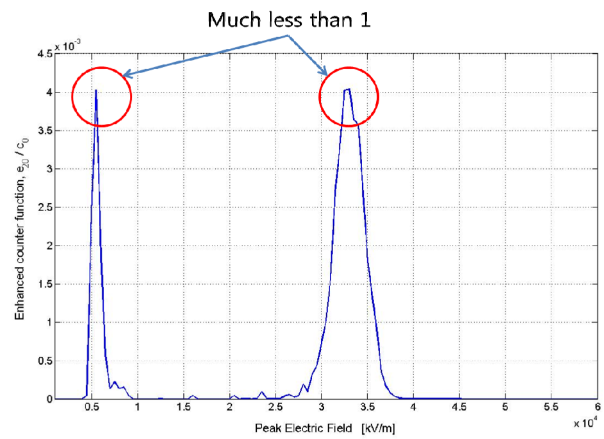

Figure 9: Enhanced counter function result.

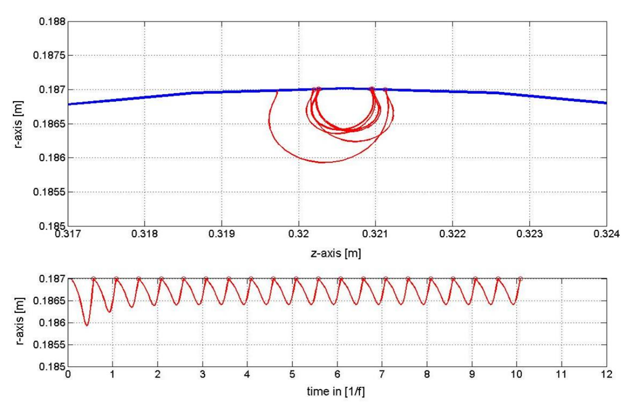

Figure 10: Electron trajectory near the equator region.

REFERENCES

[1] Sang-Ho Kim, J. Korean Phys. Soc. 54, 1925 (2009).

[2] Sun An, "Superconducting RF Cavity Frequency and Field Distribution Sensitivity Simulation," PAC'05, Knoxville, 2005, p. 4194 (2005).

[3] Han-Sung Kim, Hyeok-Jung Kwon and Yong-Sub Cho, J. Korean Phys. Soc. 56. 1989 (2010).

[4] P. Yla-Oijala, D. Proch, "Multipac – Multipacting Simulation Package with 2D FEM Field Sovler", SRF'01, Tsukuba, 2001, p. 105 (2001).

ISBN 978-3-95450-115-1